American Mineralogist, Volume 89, pages 176–184, 2004

Investigation of Al/Si ordering in tetrahedral phyllosilicate sheets by Monte Carlo simulation

ERIKA J. PALIN* AND MARTIN T. DOVE

Department of Earth Sciences, University of Cambridge, Downing Street, Cambridge CB2 3EQ, U.K.

ABSTRACT

We have investigated by Monte Carlo simulation the Al/Si ordering behavior of the tetrahedral phyllosilicate sheet, with a variety of compositions from Al_1Si_1 to Al_1Si_7, using atomic interaction parameters determined for the tetrahedral sheet in muscovite. Three different ordering schemes operate, depending on composition, with relatively Al-poor systems ordering in a muscovite-like (Al:Si = 1:3) pattern and relatively Al-rich compositions ordering in an "ABABAB" or margarite-like (Al:Si = 1:1) pattern, where ABABAB indicates the arrangement of atoms around a hexagonal ring of tetrahedral cation sites. The pattern corresponding to Al:Si = 1:2 occurs in intermediate compositions, but always in conjunction with another ordering pattern, except for one composition close to Al:Si = 1:2. Simulations of the same composition but with different ordering schemes can show different behavior, and this is evidence for metastability fields. The transition temperature for order-disorder T_c is strongly dependent on composition, and the dilution effect can be observed at low Al concentrations, with a critical concentration x_c between 0.12 and 0.15.

INTRODUCTION

The tetrahedral sheet in phyllosilicate minerals can exhibit a variety of compositions depending on the mineral. Examples include Al:Si = 1:3 in muscovite, 1:7 in phengite, and 1:1 in margarite. In previous work, we have investigated the ordering behavior of the tetrahedral sheet in muscovite (Palin et al. 2001), of the tetrahedral and octahedral sheets in phengite (Palin et al. 2003a), and of the octahedral sheet in other phyllosilicate minerals such as illites and smectites (Sainz-Díaz et al. 2003a,b; Palin et al. 2004). Here, we address the issue of ordering in the tetrahedral sheet in a more general fashion than in our previous muscovite work. We investigate by Monte Carlo simulation a variety of compositions, from very dilute systems up to a 1:1 ratio of Al:Si, to determine both the degree of order that is present and the nature of the ordering scheme, to observe the effect of variation in concentration.

A previous computational study (Myers et al. 1998) of Al/Al avoidance in aluminosilicate structures, including the feldspar and cordierite frameworks, compared the behavior of these systems with the Bragg-Williams model of cation ordering. Figure 1 shows schematically the observed behavior as compared with the model. The value of x at which T_c falls to zero is called the critical concentration, x_c. The Bragg-Williams model predicts that $x_c = 0$, whereas in real systems it has been found that there is a dramatic fall in T_c with decreasing Al content x, such that x_c can be considerably greater than zero. This is because the Bragg-Williams model does not account for short-range order, and in reality, Al/Al avoidance can occur without short-range order driving the formation of long-range order. This effect was termed the "dilution effect," and has been cited as the reason for the low transition temperatures in systems such as leucite (Dove et al. 1993), and we have observed further evidence for the effect in our studies of phengite (Palin et al. 2003a) and octahedral illite/smectite sheets (Sainz-Díaz et al. 2003a,b).

It is instructive to study many different compositions of the tetrahedral sheet due to the very wide compositional variation in natural phyllosilicate minerals. In this work, we build on the previous work by Myers et al. (1998), who showed that two controls on the value of x_c are the dimensionality of the system and the coordination number of the atoms. The tetrahedral sheet is an interesting case with respect to both of these factors; it is essentially two-dimensional, and the atoms have a relatively low nearest-neighbor coordination number of three. More importantly, the previous study considered only nearest-neighbor interactions, thereby allowing investigation of only one ordering scheme, whereas in this work we will consider interactions between more distant pairs, which allow for the possibility of up to three different possible ordering schemes. Thus we are able to extend the analysis of Myers et al. (1998) to include the effects of competing ordering schemes.

METHOD

The method employed in this work has been discussed in detail in other papers (Bosenick et al. 2001; Warren et al. 2001). Briefly, we first calculate atomic interaction parameters using lattice energy minimization methods and empirical interatomic potentials, and then use these atomic interaction parameters in Monte Carlo (MC) simulations of ordering.

In this work, we use previously calculated values of the atomic interaction parameters that we determined for the tetrahedral sheet in muscovite. The full details are given in Palin et al. (2001). The first stage of the calculation of the atomic interaction parameters involved building a model of the muscovite structure, parameterized using empirical interatomic potentials. The formulae for these potentials, and the values used for the various different types of atoms, are given in Appendix 1.

The lattice energy of the model was minimized using the program GULP (Gale 1997). Initially, a disordered model was used, employing the virtual crystal approximation, whereby all the tetrahedral sites in the muscovite structure are occupied with a virtual atom consisting of 0.25Al + 0.75Si to represent disorder. The resulting optimized structure showed good agreement when compared with an experimentally determined muscovite structure (Catti et al. 1994): the differences between experimental and model lattice parameters were less than 1.5%, and the mean interatomic distances agreed to within 1% (O-H and octahedral

* E-mail: ejp24@cam.ac.uk

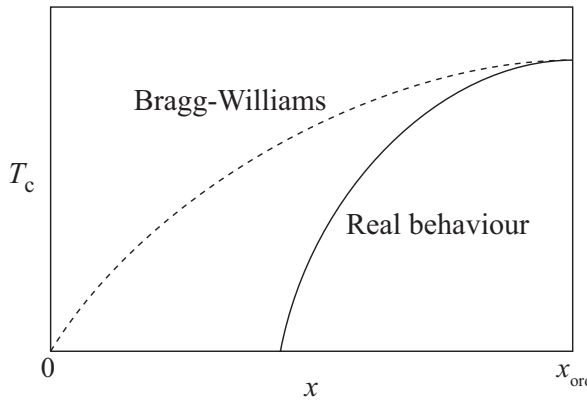

FIGURE 1. Schematic behavior of transition temperature T_c with Al concentration x compared with that predicted by the Bragg-Williams model (after Myers et al. 1998). The right-hand limit, x_{ord}, corresponds to the value of x for the fully ordered case (which need not be for a 1:1 ratio).

Al-O to within 3%).

The parameters from the optimized disordered structure were then used as input parameters for a set of model structures in which the Al and Si atoms were localized at random tetrahedral sites (with the constraint that charge balance in each T-O-T layer was preserved). Fifty configurations of this form were thus generated, and each of these was optimized using GULP.

The model Hamiltonian we used to determine the atomic interaction parameters J_n is given by

$$E = E_0 + \sum_n N^n_{\text{Al–Al}} J_n \quad (1)$$

where E is the lattice energy of a configuration, given by GULP, E_0 is a constant term that does not affect the ordering process, $N_{\text{Al–Al}}$ is the number of Al-Al interactions in a particular configuration for a particular distance, and J is the atomic interaction parameter between atoms separated by a particular distance. Equation 1 is a simple linear equation, and as such, we obtain values for E_0 and the Js by linear regression of the fifty E values from GULP against the fifty sets of $N_{\text{Al–Al}}$ values, with the latter quantity being calculated for each interaction parameter for each configuration using a spreadsheet.

The distances corresponding to the J parameters are shown in Figure 2; they represent nearest-neighbor tetrahedral sites, next-nearest, third-nearest, and fourth-nearest sites within one tetrahedral sheet. The values calculated using the regression method described above are given in Table 1.

We used our own code, Ossia, for the MC simulations. Details are available from http://www.esc.cam.ac.uk/ossia. Temperature is incorporated into the MC simulations by use of the Metropolis algorithm; one iteration step of the Monte Carlo process can be described as follows. Two atoms within the simulation box are selected at random and swapped. The energies of the configuration before and after the swap are compared. If the swap results in a decrease in energy the new configuration is retained and the next iteration step follows. If the energy increases as a result of the swap, however, the swap is retained subject only to a probability test:

$$P(E \rightarrow E + \Delta E) = \exp(-\Delta E/k_B T) \quad (2)$$

and the next iteration step follows. The Boltzmann factor contained in the probability test will have a different value for each simulation temperature, and hence different structures will occur with different probabilities at different temperatures. The MC process begins with an initial simulation in which the system relaxes to equilibrium. The production experiment follows this, and has the same number of iteration steps as the equilibration component, with averages (from which thermodynamic quantities are determined) being taken every 500 steps. Typically, the production experiment uses up to 10^8 iteration steps (that is, 2×10^8 steps including the equilibration experiment) to ensure good statistics. In this study we used 200 million iteration steps in the production component and performed simulations at twenty different temperatures for each composition studied. In some cases, further simulations were performed over narrower temperature ranges to examine behavior near phase transitions.

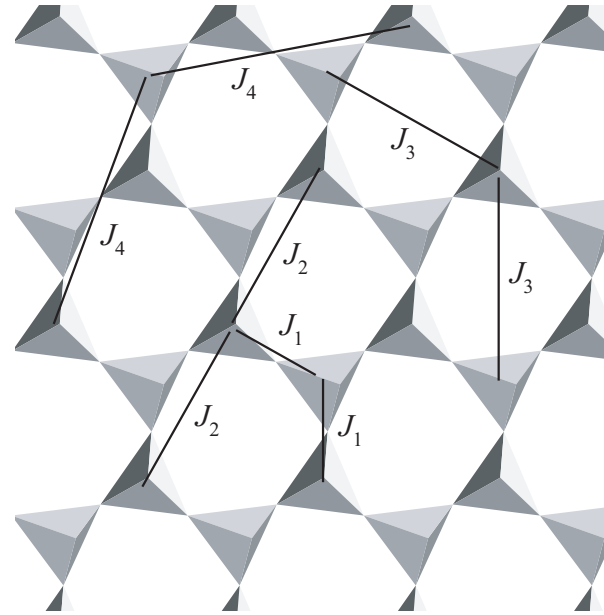

FIGURE 2. Distances within the tetrahedral sheet corresponding to J parameters (values for which are given in Table 1).

TABLE 1. Values of atomic interaction parameters J_n determined for muscovite (Palin et al. 2001)

Parameter	Distance (Å)	Value (eV)
J_1	2.97–3.08	1.0(1)
J_2	5.22	0.23(5)
J_3	5.96–6.05	0.00(5)
J_4	7.92–8.04	0.13(4)

Usually, we use Ossia to simulate ordering in one of two ways: either a "hot start," starting the system from a random configuration and decreasing the temperature to monitor ordering, or a "cold start," starting the system from an ordered state and increasing the temperature to monitor disordering. However, in this work we sampled a variety of compositions with respect to three particular ordering schemes. The ordering schemes are illustrated in Figure 3; it can be seen that they correspond to three specific compositions of the tetrahedral sheet (Al:Si = 1:3, hereafter referred to as the "muscovite scheme"; Al:Si = 1:1, hereafter referred to as the "margarite scheme"; Al:Si = 1:2, hereafter referred to as the "1:2 scheme"). This fact means that neither of our usual approaches is viable, because the majority of compositions we study are obviously not identical to the ordered states corresponding to these order parameters.

Therefore, in this work, we used a feature of the code that we previously used in our phengite work (Palin et al. 2003a); that is, the ability to simulate partial ordering, and we call this a "warm start." The method is similar to that for a cold start, except that in the initial ordered state, atoms of one type are swapped at random to atoms of the other, until the desired fractions of atoms are obtained. Thus we have a mixture of order and disorder simultaneously. The simulation then proceeds as would a normal cold start simulation.

It should be stressed that the system is not constrained to remain in the starting configuration once the atomic fractions have been changed. On some occasions, this will occur, but it is obvious from the energy data for the system if this is energetically unfavorable, because the energy will undergo an initial decrease on heating before it increases.

We performed simulations on the following compositions (fractions of Al, x, are in 64^{ths} for ease of comparison): Al-poor: x = 8/64 (phengite composition) – 16/64 (muscovite composition); Intermediate: x = 18/64 – 24/64; Al-rich: x = 26/64 – 32/64 (margarite composition).

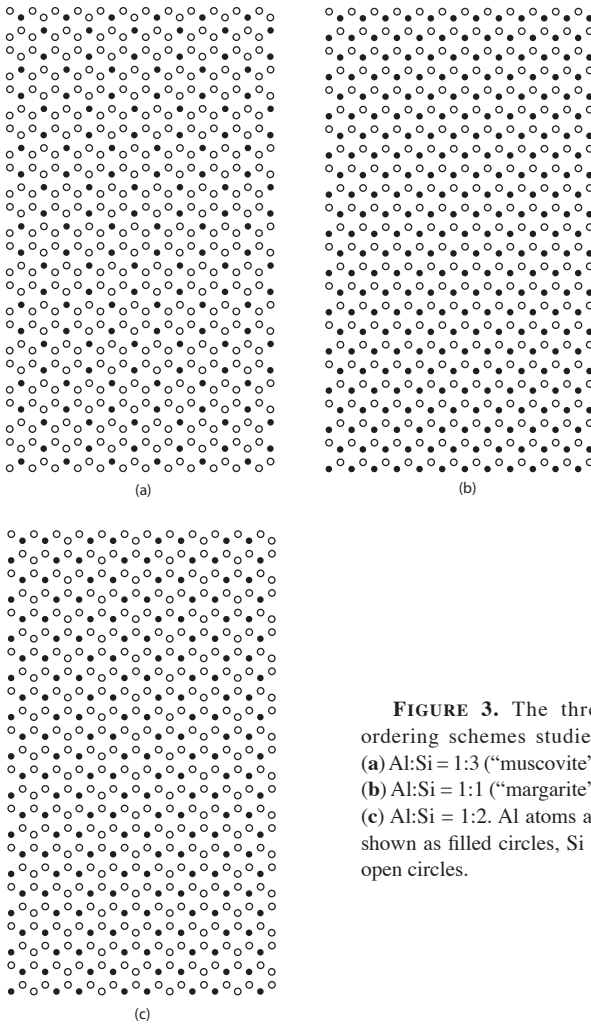

FIGURE 3. The three ordering schemes studied: (**a**) Al:Si = 1:3 ("muscovite"), (**b**) Al:Si = 1:1 ("margarite"), (**c**) Al:Si = 1:2. Al atoms are shown as filled circles, Si as open circles.

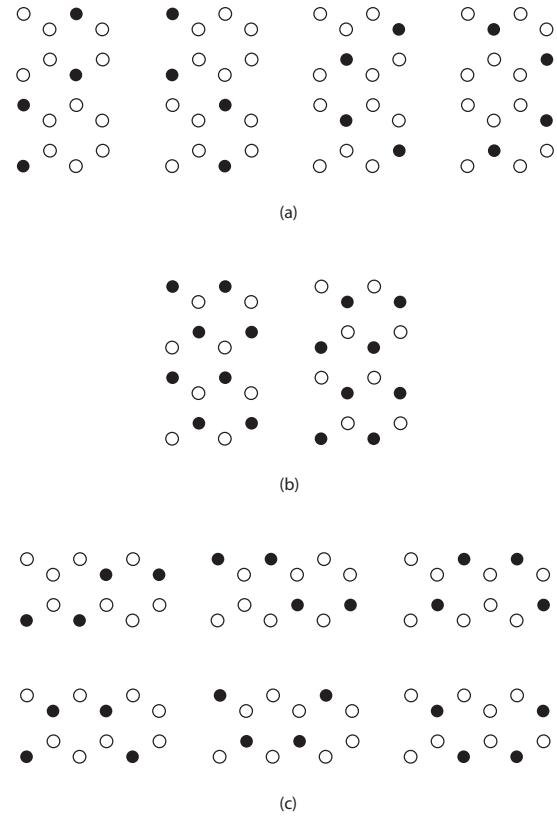

FIGURE 4. Different arrangements of each ordering scheme with respect to the unit cell used. (**a**) Muscovite scheme, (**b**) margarite scheme, (**c**) 1:2 scheme. Al atoms are shown as filled circles, Si as open circles.

For Al-poor systems, we used the muscovite ordered scheme as the starting configuration, and for the intermediate and Al-rich compositions we performed simulations starting with all three schemes. Our justification for using the margarite scheme for the Al-rich systems is that in previous studies of different cation systems, we have found that the same pattern exists for A:B = 1:1 (e.g., octahedral phyllosilicate sheets containing any of Al:Fe = 1:1, Al:Mg = 1:1, Fe:Mg = 1:1—see Sainz-Díaz et al. 2003a,b). We used the 1:2 scheme for interest; it is a possible tetrahedral composition in trioctahedral micas such as biotite, but less likely in dioctahedral micas.

The order parameters are set up by declaring the expected pattern of atoms at sites for each order parameter. Then, the order parameter is measured by considering how many sites are occupied by the expected atoms. If, for a given site, the occupancy of one type of cation at that site averaged over all unit cells is s_j, then $s_{j,0}$ is the average occupancy of the ordered structure (i.e., at $T = 0$) and $s_{j,\infty}$ is the average occupancy as $T \to \infty$. The order parameter per site is then defined as

$$Q_j = \frac{s_j - s_{j,\infty}}{s_{j,0} - s_{j,\infty}} \quad (3)$$

The disordered occupancies $s_{j,\infty}$ are calculated as random averages of all the cations used in the simulation—for example, for an A:B = 1:3 ratio, the random occupancy of a site would be $A_{0.25}B_{0.75}$. The overall order parameter is simply a normalized sum of the site order parameters over all sites in all unit cells in the simulation box.

For the muscovite scheme, there are four possible arrangements of the atoms with respect to the unit cell (see Fig. 4a), and hence all of these must be declared. For the margarite scheme, there are two possible arrangements of the atoms with respect to the unit cell (see Fig. 4b). However, only one order parameter needs to be declared, because one configuration is simply the anti-ordered version of the other, and hence a configuration with order parameter Q is simply the anti-ordered version of a configuration with order parameter $-Q$.

For the 1:2 scheme, a different unit cell must be used; in this case there are six possible arrangements of the atoms with respect to the unit cell (Fig. 4c), each of which must again be declared.

Therefore each simulation has either five order parameters, Q_1 for the margarite scheme, and Q_{2-5} for the four possible configurations of the muscovite scheme; or six order parameters, Q_{6-11} for the six possible configurations of the 1:2 scheme.

The simulation boxes we used were $8 \times 8 \times 1$ multiples of the 16-site and 12-site cells shown in Figure 4. Each simulation box therefore contained 1024 tetrahedral sites (muscovite and margarite schemes) or 768 tetrahedral sites (1:2 scheme); a simulation box of this size is sufficient to avoid the problem of size effects.

To enable comparisons between all systems, some transformations were performed on the raw order parameter data. For the margarite scheme, we simply took the absolute value of Q_1, for the reasons described above. For the muscovite scheme, the values of the square root of the sum of squares of the order parameter were computed for each temperature. For perfect order, i.e., for x = 16/64, we expected the order parameters Q_{2-5} to be 1, –1/3, –1/3, –1/3 (or some combination thereof), and hence the square root of the sum of squares is $\sqrt{4/3}$. Then, all values of the square root of the sum of squares for other systems were normalized by this factor, and we called this new normalized order parameter Q_{musc}. For the 1:2 scheme, we performed a similar analysis: for perfect order, we expected the order parameters Q_{6-11} to be 1, –1/2, –1/2, –1/2, 1/4, 1/4 (or some combination thereof) and hence the normalizing factor is $\sqrt{15/8}$. The normalized order parameter was then called $Q_{1:2}$.

The energies and order parameters output from the simulations can be used to give further useful information in the form of the heat capacity C and susceptibility χ, which are calculated from fluctuations in the energy and order parameter respectively:

$$C = \frac{\langle E^2 \rangle - \langle E \rangle^2}{k_B T^2} \quad (4)$$

$$\chi = \frac{\langle Q^2 \rangle - \langle Q \rangle^2}{k_B T} \quad (5)$$

RESULTS

We present here a selection of results from the compositions studied. Full data sets are available on the internet at http://www.esc.cam.ac.uk/minsci/downloads/AlSiord/.

Al-poor systems

Plots of Q_{musc} for the Al-poor systems are shown in Figure 5a. Three things can be seen from this figure: (1) for compositions above approximately $x = 12/64$, the order parameter at low temperature has a well-constrained value, and the point at which it decreases to zero is relatively well-defined. At compositions below this, the behavior of the order parameter becomes less clear, and it is harder to determine a value for T_c; (2) the transition temperatures decrease with decreasing Al content; this is the dilution effect, as discussed above (Dove et al. 1996; Myers et al. 1998); (3) the maximum value of the order parameter decreases with decreasing Al content; this behavior is expected, since the order parameter is set up site by site, and therefore the more "incorrect" sites there are, the lower the theoretical maximum value of Q will be.

Figure 5b shows structure snapshots for $x = 8/64$, 12/64, and 16/64. In Figure 5b(i), the dispersed nature of the Al is evident, in that the system only exhibits some short range order. In Figure 5b(ii), the long-range ordering pattern begins to become more obvious, and by the time the system is enriched in Al to the muscovite composition [Fig. 5b(iii)], long range order occurs.

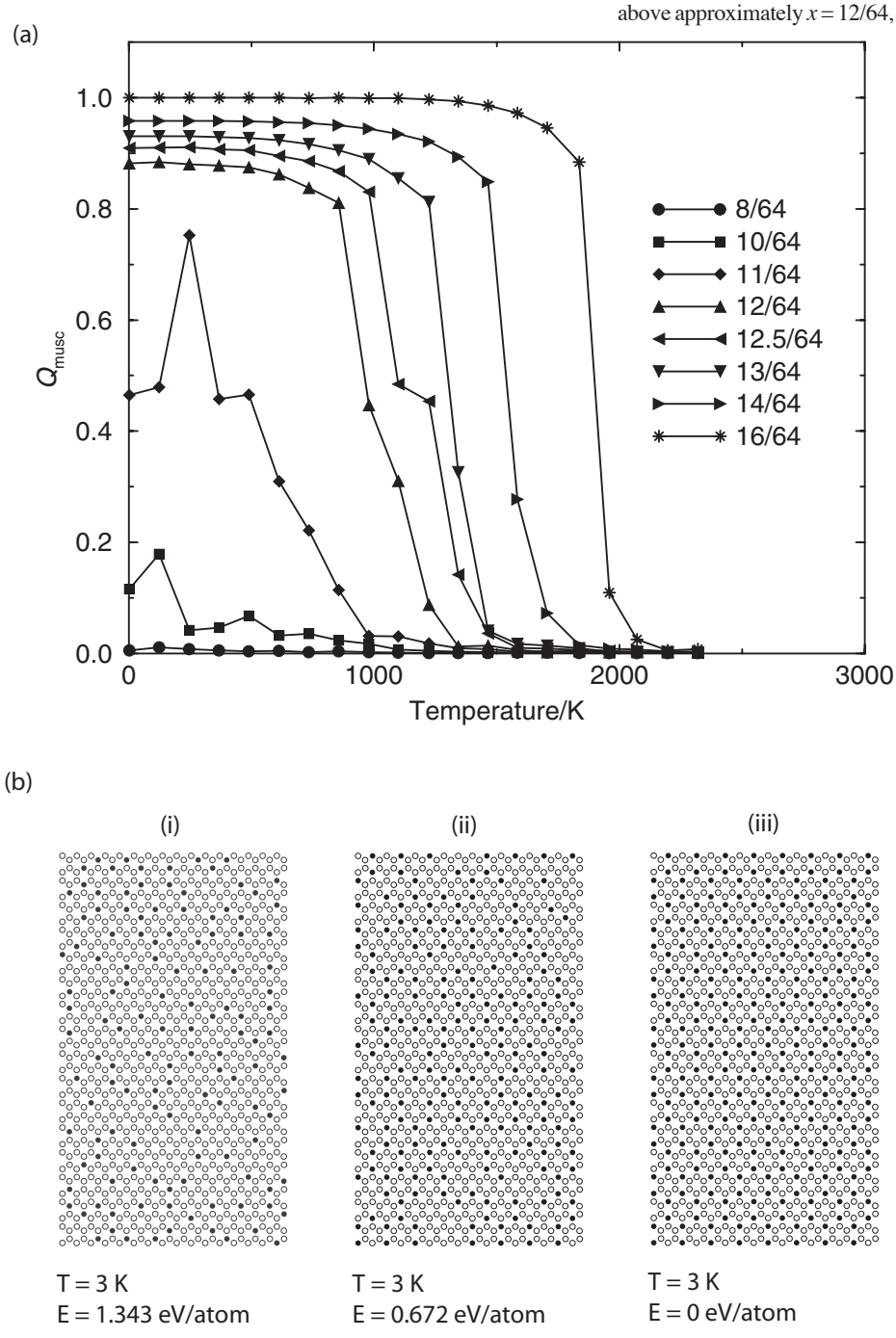

FIGURE 5. (**a**) Order parameter data (Q_{musc}) for Al-poor systems. (**b**) Structure snapshots for selected Al-poor systems: (i) 8/64, (ii) 12/64, (iii) 16/64. Filled circles represent Al and open circles Si.

Al-rich systems

The order parameter results (Q_1) for the Al-rich systems are given in Figure 6a. Once again, the effects of dilution are evident from the figure in that the systems with progressively lower Al content have progressively lower T_c values. Snapshots of $x = 26/64$ and 30/64 are shown in Figure 6b. The pattern of ordering in these systems can be viewed in two ways, either as the margarite scheme with several defects, or as a mixture of margarite and 1:2 ordering schemes—the change

from one ordered scheme to the other is continuous, since the two schemes are related by exchanging Al for Si at the centers of the hexagons formed by six Al-Al J_2 linkages.

Intermediate systems

Predicting the behavior of the intermediate systems is difficult, since it could be possible for them to order in any of the three ordering schemes studied. The order parameter behavior for intermediate compositions is shown in Figures 7a(i) (Q_1 for simulations started in the margarite scheme) and 7a(ii) (Q_{musc} for simulations started in the muscovite scheme). Snapshots of the structures for x = 22/64 and 24/64 are shown in Figure 7b, for simulations started in each of the muscovite and margarite ordering schemes. In all cases, the snapshots show a complicated mixture of ordering schemes. The two simulations started in the muscovite scheme contain some regions still ordered in this scheme, and some regions ordered in the other two schemes. However, the two simulations started in the margarite scheme only show evidence for the 1:2 and margarite schemes (with the 22/64 system started in the margarite scheme showing almost exclusively 1:2 ordering). This suggests that the muscovite scheme exists metastably at these compositions, and we will discuss this in more detail below.

Again, the order parameter graphs in Figure 7a show the dependence on composition of the maximum value of the order parameter. Equally, we can see the switch from muscovite-like to margarite-like behavior in the decreasing quality of the form of the curves for one ordering scheme with respect to the other.

We also examined the intermediate systems with respect to the 1:2 scheme. The order parameter behavior ($Q_{1:2}$) for these systems is shown in Figure 8; again T_c is composition-dependent, and the quality of the form of the curves varies. It is difficult to determine the amount of 1:2 ordering in these systems; the data in Figure 8 can show a fairly high degree of order, but this is because the 1:2 ordering scheme is simply the same as the margarite ordering scheme with some atoms removed. Hence, the 1:2 order parameters will pick up both 1:2 and margarite ordering, and the only way to determine the proportions of each is by visual inspection of the configurations. An examination of the evolution of the structure as a function of temperature shows that in all systems, most regions that are initially ordered in the 1:2 pattern are lost in favor of 1:3 and 1:1 regions. An example of this behavior is shown for x = 20/64 in Figure 9. The energy as output from the MC simulation is shown in Figure 9a. At low temperature, the configuration in Figure 9b(i), consisting of mostly 1:2 regions, is metastable. With increasing temperature, the energy gradually decreases to produce regions of 1:3 and mixed 1:1/1:2 character in Figure 9b(ii). Figure 9b(iii) shows

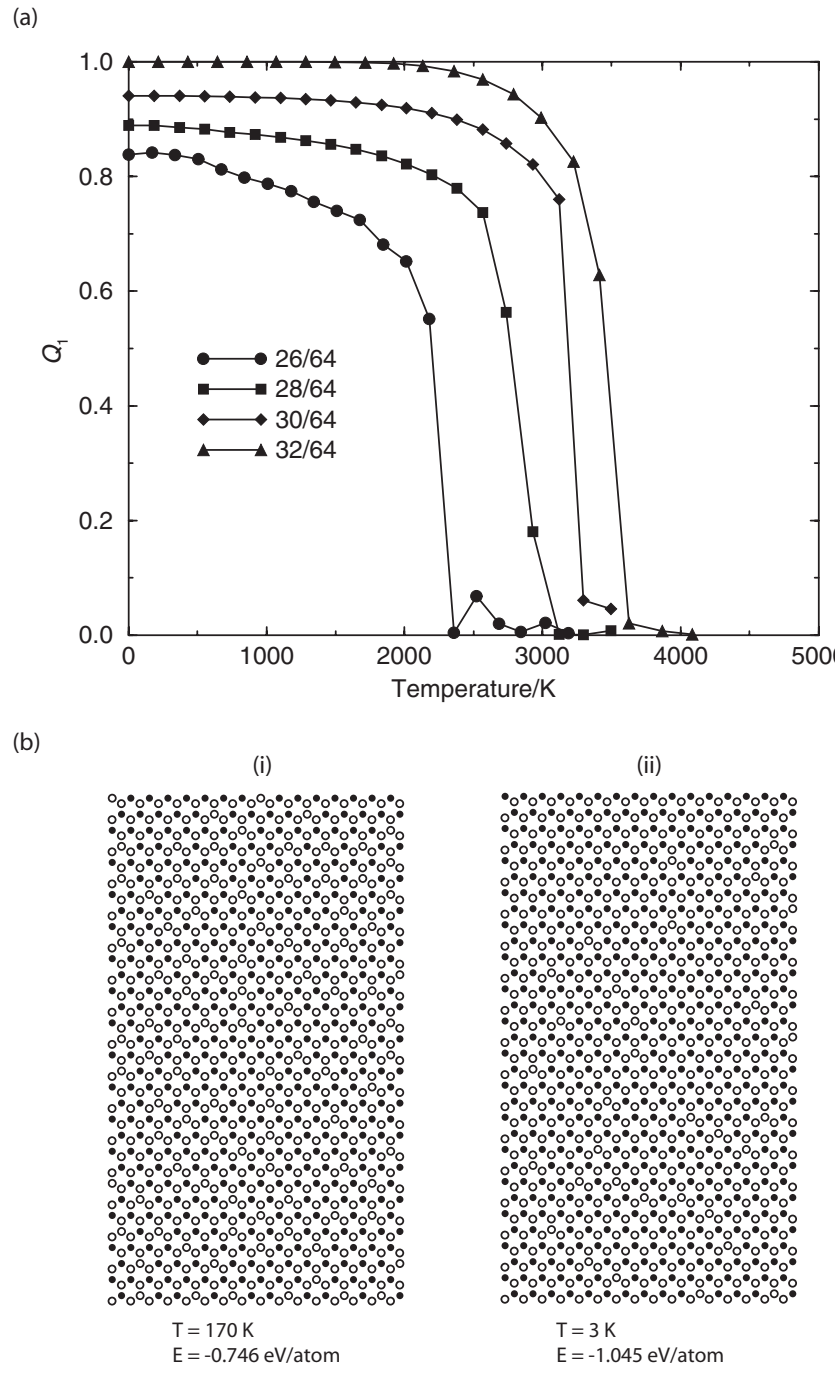

FIGURE 6. (**a**) Order parameter data (Q_1) for Al-rich systems. (**b**) Structure snapshots for selected Al-rich systems: (i) 26/64, (ii) 30/64. Filled circles represent Al and open circles Si.

the disordered structure of the system above T_c.

The splitting into 1:1 and 1:3 regions is most pronounced for the 18/64 and 20/64 compositions; at these concentrations, it is still energetically favorable for the system to split into these components, because the energy of the 1:3 configuration is essentially zero (i.e., in the case of perfect order, the only Al-Al interactions are J_3, and $J_3 \approx 0$). As the system becomes richer in Al, this becomes less pronounced, until at the 1:2 ratio it becomes energetically more preferable for the 1:2 configuration to exist. With further Al enrichment, the 1:1 scheme begins to coexist with the 1:2 scheme.

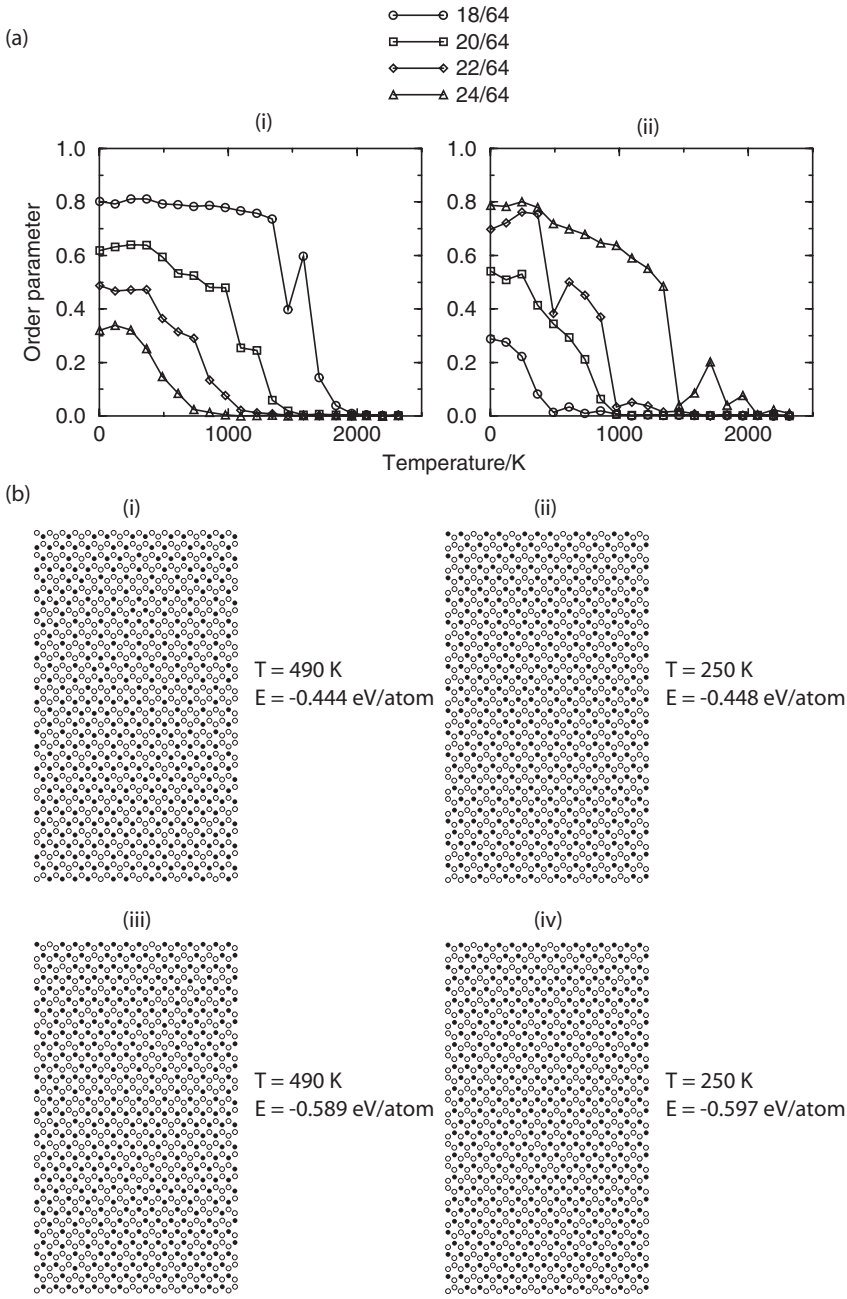

FIGURE 7. (**a**) Order parameter behaviour for intermediate compositions: (i) Q_{musc} started in the muscovite scheme, (ii) Q_1 started in the margarite scheme. (**b**) Structure snapshots for selected intermediate systems: (i) 22/64 started in the muscovite scheme, (ii) 22/64 started in the margarite scheme, (iii) 24/64 started in the muscovite scheme, (iv) 24/64 started in the margarite scheme.

DISCUSSION

Transition temperatures

Figure 10 shows a plot of T_c vs. composition for all the systems studied in this work. We can make some comments with regard to dilution; extrapolating the relationship between T_c and x for the muscovite curve back to $T_c = 0$ (i.e., the point below which no transition should be observed) gives a value for x_c of between 8/64 and 10/64, i.e., around 0.12–0.15. It is not possible to provide a more precise value because the graphs of Q at such dilute compositions do not show clear transition temperatures.

In spite of the differences between the previous study and this one, there are certain similarities between the results. Most of the Myers et al. (1998) graphs of T_c against x, for an $x = 0.5$ order parameter over the range $x = 0$–0.5, show $x_c \sim 0.3$, i.e., x_c has a value ~60% of the x value corresponding to the maximally ordered state. Our graph of T_c against x for the $x = 0.25$ (muscovite) order parameter over the range $x = 0$–0.25 shows $x_c \sim 0.15$, and hence there appears to be a similar relationship between T_c and x in both studies, whereas one might expect that our value x_c would have been closer to zero, given the extension to more distant neighbors.

Ordering schemes and metastability

In previous studies we have commented on the way in which the J values can control ordering in a strict manner. For example, in muscovite it is the value of J_4 that dictates the ordering scheme—without the inclusion of this parameter, more than one ordering scheme is possible. This is, of course, also true in this study, since we are using the muscovite J values. In this study, the noteworthy point is that with only one set of Js we can obtain three different ordered states by varying only the composition of the system.

It is interesting to note the behavior of different order parameters in Figure 10. The curves for the 1:2 and margarite order parameters cross the curve for the muscovite order parameter in the vicinity of $x = 22/64$. This value is very close to a 1:2 ratio, which is as one might expect, since it indicates that

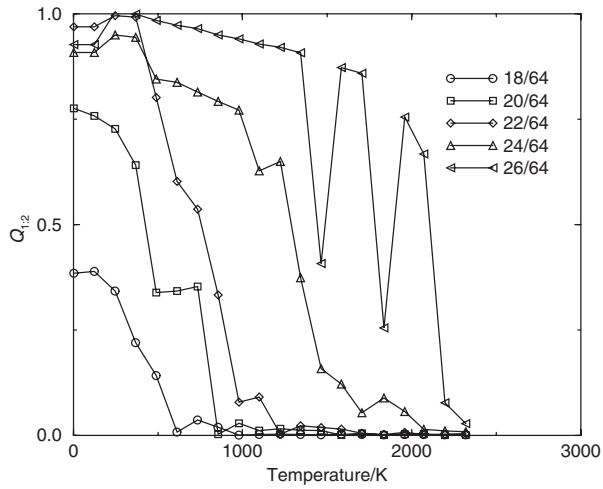

FIGURE 8. Order parameter data ($Q_{1:2}$) for intermediate systems. The two anomalously low points for 26/64 are due to the existence of domain structures.

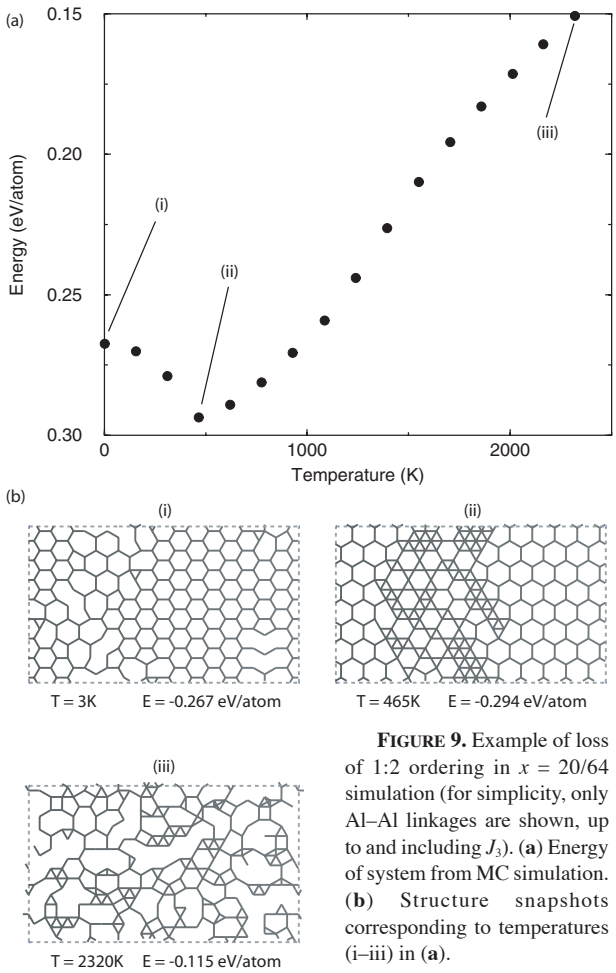

FIGURE 9. Example of loss of 1:2 ordering in x = 20/64 simulation (for simplicity, only Al–Al linkages are shown, up to and including J_3). (**a**) Energy of system from MC simulation. (**b**) Structure snapshots corresponding to temperatures (i–iii) in (**a**).

the stable configuration switches from the muscovite scheme to the margarite scheme at this value. The simulations started in the 1:2 ordering scheme are interesting in that the temperature

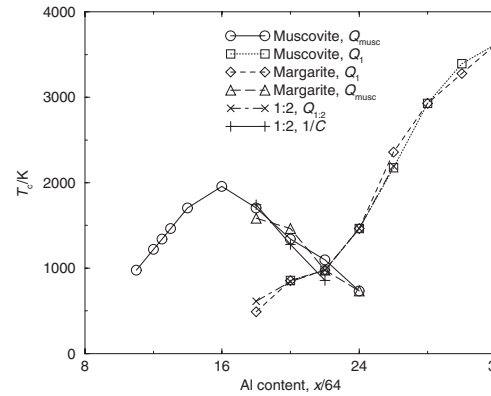

FIGURE 10. Plot of transition temperatures T_c against Al content x. Each curve is labeled with the initial configuration and the property measured, e.g., "Muscovite, Q_{musc}" indicates the simulation was started in the muscovite scheme and the temperature shown is that at which Q_{musc} becomes zero (except for the $1/C$ curve, where temperature shown is the minimum value of $1/C$).

at which Q decreases to zero is not always the same as that at which the heat capacity diverges (i.e., the point at which $1/C$ reaches a minimum). Figure 10 shows that the $Q_{1:2}$ order parameter values increase with increasing x, but the heat capacity anomaly temperature decreases with increasing x. The $Q_{1:2} = 0$ curve coincides approximately with the curves for $Q_1 = 0$ over a similar range of x, whilst heat capacity anomaly data coincide approximately with the data for $Q_{musc} = 0$ over a similar range of x. This is because at higher x, both Q_1 and $Q_{1:2}$ will record margarite-like behavior, since the 1:2 and margarite schemes are closely related; whilst at lower x, there will be more muscovite-like regions whose behavior will be recorded by Q_{musc}.

Figure 10 also shows evidence for metastability fields. Between x = 18/64 and 22/64, the muscovite order parameter curves occur at higher temperature than those for margarite, indicating that muscovite is stable, but margarite is metastable—that is, in this compositional range, a simulation started in the margarite scheme would persist in that scheme until a certain temperature was reached, whereupon the system would be expected to convert to the muscovite scheme before disordering. Above x = 22/64, the opposite is true. Figure 11 shows order parameter data for x = 18/64 (started in margarite scheme) and 24/64 (started in muscovite scheme). In both cases, the switch from one scheme to another is represented by the increase in the values of one order parameter at the expense of the other. In the first case, the margarite pattern persists up to approximately 490 K before the ordering switches to the muscovite pattern. In the second case, the muscovite pattern persists up to ~740 K before ordering switches to the margarite pattern.

Comparison of simulated behavior with experimental behavior

In previous studies (e.g., Palin et al. 2001) we have noted that the behavior shown by our simulations does not necessarily agree exactly with the ordering behavior shown by experimental investigations. In particular, long range order is rarely detected experimentally in phyllosilicates. We attribute this to the fact that real systems are influenced not only by thermodynamics,

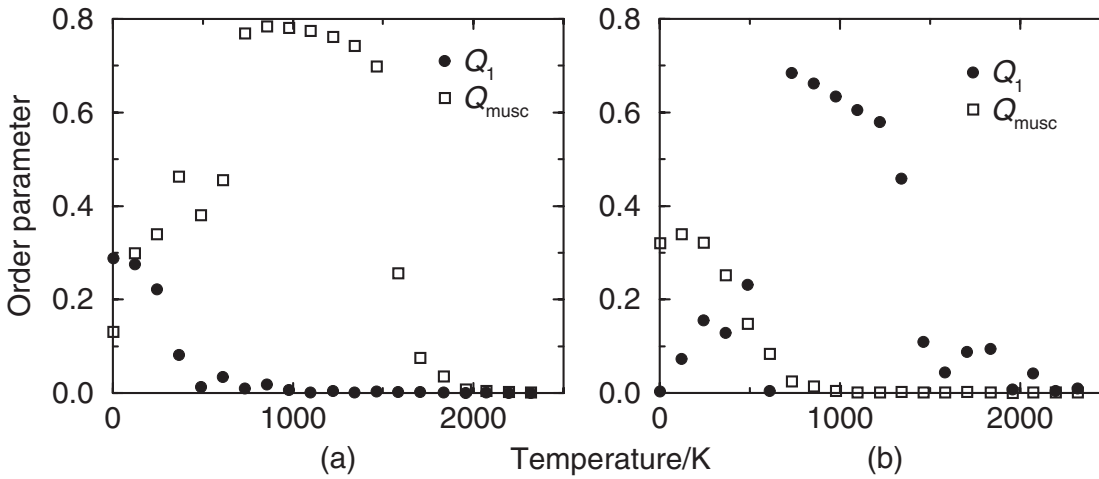

FIGURE 11. Examples of evidence for metastability in compositions (**a**) x = 18/64 and (**b**) x = 24/64.

but also by kinetics. MC simulations are based only on thermodynamics, without the incorporation of any time component, and hence cannot give kinetic information. This means any long-range-ordered states shown by our simulations may only rarely be attained in nature. Nonetheless, the MC simulations still provide insights into the possible behavior of real phyllosilicate samples, and as such could be of geological interest, given the compositional range we have covered and the wide range of naturally occurring phyllosilicate compositions. In spite of the lack of a kinetic component in the simulations, the suggested regions of metastability we have determined occur at common phyllosilicate compositions and at geological temperatures. This could be important in geological systems, which are often not at thermodynamic equilibrium.

ACKNOWLEDGMENTS

E.J.P. is grateful to EPSRC for financial assistance and to W. Lee for helpful discussions. The Monte Carlo simulations were performed on the Mineral Physics Group's Beowulf cluster at the Department of Earth Sciences, University of Cambridge. The simulations used a pseudo-random number generating routine written by R. Chandler (UCL) and P. Northrop (Oxford).

REFERENCES CITED

Bosenick, A., Dove, M.T., Myers, E.R., Palin, E.J., Sainz-Díaz, C.I., Guiton, B., Warren, M.C., Craig, M.S., and Redfern, S.A.T. (2001) Computational methods for the study of energies of cation distributions: applications to cation-ordering phase transitions and solid solutions. Mineralogical Magazine, 65, 193–219.

Catti, M., Ferraris, G., Hull, S., and Pavese, A. (1994) Powder diffraction study of $2M_1$ muscovite at room pressure and at 2 GPa. European Journal of Mineralogy, 6, 171–178.

Dove, M.T., Cool, T., Palmer, D.C., Putnis, A., Salje, E.K.H., and Winkler, B. (1993) On the role of Al-Si ordering in the cubic-tetragonal phase transition of leucite. American Mineralogist, 78, 486–492.

Dove, M.T., Thayaparam, S., Heine, V., and Hammonds, K. (1996) The phenomenon of low Al/Si ordering temperatures in aluminosilicate framework structures. American Mineralogist, 81, 349–362.

Gale, J.D. (1997) GULP: a computer program for the symmetry-adapted simulation of solids. Journal of the Chemical Society - Faraday Transactions, 93, 629–637.

Myers, E.R., Heine, V., and Dove, M.T. (1998) Thermodynamics of Al/Al avoidance in the ordering of Al/Si tetrahedral framework structures. Physics and Chemistry of Minerals, 25, 457–464.

Palin, E.J., Dove, M.T., Redfern, S.A.T., Bosenick, A., Sainz-Díaz, C.I., and Warren, M.C. (2001) Computational study of tetrahedral Al–Si ordering in muscovite. Physics and Chemistry of Minerals, 28, 534–544.

Palin, E.J., Dove, M.T., Redfern, S.A.T., Sainz-Díaz, C.I., and Lee, W.T. (2003a) Computational study of tetrahedral Al–Si and octahedral Al–Mg ordering in phengite. Physics and Chemistry of Minerals, 30, 293–304.

Palin, E.J., Dove, M.T., Sainz-Díaz, C.I., and Hernández-Laguna, A. (2004) A computational investigation of the Al/Fe/Mg order-disorder behaviour in the dioctahedral sheet of phyllosilicates. American Mineralogist, 89, 165–176.

Sainz-Díaz, C.I., Palin, E.J., Hernández-Laguna, A., and Dove, M.T. (2003) Octahedral cation ordering of illite and smectite. Theoretical exchange potential determination and Monte Carlo simulations. Physics and Chemistry of Minerals, 30, 382–392.

Sainz-Díaz, C.I., Palin, E.J., Dove, M.T., and Hernández-Laguna, A. (2003b) Ordering of Al, Fe and Mg cations in the octahedral sheet of smectites and illites by means of Monte Carlo simulations. American Mineralogist, 88,1033–1045.

Warren, M.C., Dove, M.T., Myers, E.R., Bosenick, A., Palin, E.J., Sainz-Díaz, C.I., Guiton, B., and Redfern, S.A.T. (2001) Monte Carlo methods for the study of cation ordering in minerals. Mineralogical Magazine, 65, 221–248.

MANUSCRIPT RECEIVED FEBRUARY 1, 2003
MANUSCRIPT ACCEPTED MAY 6, 2003
MANUSCRIPT HANDLED BY MARIA BRIGATTI

Continued next page

APPENDIX 1. EMPIRICAL INTERATOMIC POTENTIALS

The model interatomic potentials used to parameterize the muscovite model are given here. For further discussion of the method used, please see Palin et al. (2001).

In the following formulae, we use the following general symbols: E to represent energy, r to represent an interatomic distance, and θ to represent an angle between two interatomic vectors. A zero subscript indicates an equilibrium value. All ions are modeled using formal charges except the hydroxyl ions, although the charges on the hydroxyl group still sum to the formal value of $-1e$.Short-range Si-O, Al-O, K-O, and O-O interactions are modeled by Buckingham energy potentials:

$$E = A\exp(-r/\rho) - Cr^{-6} \quad \text{(A.1)}$$

For Al-O and K-O, C has zero value. O-Si-O tetrahedral and O-Al-O tetrahedral and octahedral interactions are modeled by three-body potentials:

$$E = \frac{1}{2}k(\theta - \theta_0)^2 \quad \text{(A.2)}$$

O-H interactions within the hydroxyl groups are modeled by a Morse potential:

$$E = D\left[\left(1 - \exp\left[-a(r - r_0)\right]\right)^2 - 1\right] \quad \text{(A.3)}$$

All O atoms except those forming part of the hydroxyl groups are modeled by the shell model, where atoms are considered to consist of a core comprising the nucleus and tightly bound inner electrons, surrounded by a massless shell of outer electrons. The cores are assigned a charge of $+0.84819e$ and the shells a charge of $-2.84819e$, maintaining the formal value for the overall charge of $-2e$. The core and shell are held together by a harmonic core-shell interaction:

$$E = \frac{1}{2}Kd^2 \quad \text{(A.4)}$$

where d is the core-shell separation.

TABLE A1A. Parameter values used in interatomic potentials, the equations for which are given in Equations A.1–A.4

Potential type	Atoms	Parameter values			
		A	*r*	*C*	r_{max}
Buckingham	Si core – O1 core	999.9	0.3012	0	8
Buckingham	Si core – O2 shell	1283.9077	0.3205	10.66	8
Buckingham	Al core – O1 core	1142.6772	0.29912	0	8
Buckingham	Al core – O2 shell	1460.3	0.29912	0	8
Buckingham	K core – O shell	65269.7	0.213	0	8
Buckingham	O shell – O shell	22764	0.149	27.88	8
Buckingham	H core – O2 shell	325	0.25	0	8

TABLE A1B. Parameter values used in interatomic potentials, the equations for which are given in Equations A.1–A.4

Potential type	Atoms	Parameter values				
		D	*a*	r_0	r_{max}	*K*
Morse	O1 core – H core	7.0525	2.1986	0.9485	1.4	
Spring (core–shell)	O core – O shell					74.92

TABLE A1C. Parameter values used in interatomic potentials, the equations for which are given in Equations A.1–A.4

Potential type	Atoms	Parameter values				
		k	θ_0	r_{max}(1–2)	r_{max}(2–3)	r_{max}(1–3)
Three-body	O shell – Al1 core – O shell	2.0974	109.47	1.8	1.8	3.2
Three-body	O shell – Si core – O shell	2.0974	109.47	1.8	1.8	3.2
Three-body	O shell – Al2 core – O shell	2.0974	90	2.2	2.2	3.2